Imaging Sub Basalt Mesozoics Along Jakhau-Mandvi and Mandvi-Mundra Profiles in Kutch Sedimentary Basin from Seismic and Gravity Modeling

ASSSRS Prasad, Kalachand Sain and Mrinal K. Sen

CSIR-National Geophysical Research Institute, Uppal Road, Hyderabad - 500007

Corresponding author's email: kalachandsain@yahoo.com

Abstract

2-D travel time inversion of first arrival and wide-angle reflection data acquired along the Jakhau-Mandvi and Mandvi-Mundra profiles in the Kutch basin have been carried out. It has brought out a five layer velocity model with average interval velocities of 2.0, 4.6, 3.2, 5.3, and 3.5 km/s above the Archean basement (5.9 km/s) along Jakhau-Mandvi profile and a four layer velocity model along Mandvi-Mundra profile with average interval velocities of 2.0, 4.65, 3.1, and 5.2 km/s above the Archean basement (5.95 km/s). The layers may correspond to the Tertiary sediments, Late Cretaceous Deccan basalt, Early Cretaceous sediments, Late Jurassic Limestone, and Early Jurassic sediments. The Early Cretaceous sediments with varying thickness (1.0-2.0 km) below 0.25 to 0.6 km Deccan basalt in the Jakhau-Mandvi region have been delineated. The Early Jurassic sediments of 0.7 to 1.2 km thickness have also been delineated along the Jakhau-Mandvi profile below the Limestone formation. This layer is found to be thinning towards Mandvi, and is not traceable along the Mandvi-Mundra profile. However, a uniformly thicker (1.75-2.0 km) Early Cretaceous sediments has been delineated below the basalt flow along the Mandvi-Mundra profile. A regionally extending Median High is found to pass through the middle part of the Mandvi-Mundra profile. This is imaged as a deep seated structure with significant hump in the basement and upwarping in the overlying sedimentary formations. Finally the seismically derived structure has been assessed by gravity modeling along the lines.

Introduction

Half of the global oil is found in Mesozoic sediments. In our country, a vast tract of Mesozoics is hidden below the basalt flow that has made the standard reflection profiling incapable of probing them due to contamination of near-vertical primary seismic waves with multiples, mode conversion and scattering waves generated by interbeds, breccia and vesicles within the basalt. The effect of these noises becomes less prominent as the source-receiver offset increases, and the primaries carrying sub-surface information stand out at the wide-angle range. Travel time inversion of wide-angle seismic data including both first arrivals and identifiable wide-angle reflected phases has been able to derive the large-wavelength velocity structure of basalt-covered sedimentary formations in the Saurashtra, central India and Mahanadi basins (Sain and Reddy, 1995; Sain and Kaila, 1996; Sain et al., 2002a, b; Sridhar et al., 2009). The Kutch basin in the western India is one of the Indian basins that has considerably thick Mesozoic sediments hidden below the Late Cretaceous Deccan basalt. The Controlled Source Seismology (CSS) group of CSIR-National Geophysical Research Institute (NGRI) acquired seismic refraction/wide angle reflection data along 72 km long Jakhau-Mandvi (NW-SE) and 57 km long Mandvi-Mundra (W-E) profiles in the Kutch basin for the exploration of sub-basalt Mesozoics in 1996-97 (Fig.1). Recently, Prasad et al. (2010) delineated 2-D shallow velocity structure along the said profiles by forward modeling (Rayamp-PC, 1987) of first arrival travel times only. They have also used the 'skip' phenomenon to map the Mesozoic sediments below the basalt cover. Here we have picked the travel times of both first arrivals with 'skips' and identifiable wide-angle reflected phases, and inverted those simultaneously as has been carried out in the Saurashtra peninsula, Mahanadi delta and central India for sub-basalt imaging (Sain et al., 2002a, b; Sridhar et al., 2009) using RayInvr Program of Zelt and Smith (1992) to obtain better constraints on both the velocity and boundary structures. Gravity modeling was also performed to assess whether the seismically derived velocity-structure can explain other geophysical data like gravity.

Basin History

The Kutch represents the northernmost part of the Atlantic type, western passive margin of India and lies close to the western convergent boundary of the Indian plate with Eurasian plate (Besse and Courtillot, 1988). Kutch is a pericontinental basin between subsurface ridge of Nagar-Parkar in the north, Radhapur arch in the east, and Kathiawar uplift in the south (Biswas, 1987; Malik et al., 2000). The basin is filled with sediments ranging in age between middle Jurassic and Holocene. The Deccan basalts of Late Cretaceous age sratigraphically divided the sedimentary formations into Tertiary, Early Cretaceous, Late Jurassic and Early Jurassic sections. The Mesozoic sediments (more than 2.4 km thick) fill the major part of the basin whereas the Tertiary sediments (more than 300 m thick) are present in the outer parts of the basin bordering the Mesozoic uplift (Biswas, 1982). The Kutch, Cambay and Narmada basins are three major marginal rift basins in the western margin platform of the Indian craton. The basins occur close to each other in the mid western part of the Indian continent. These basins are bounded by intersecting faults whose trends follow

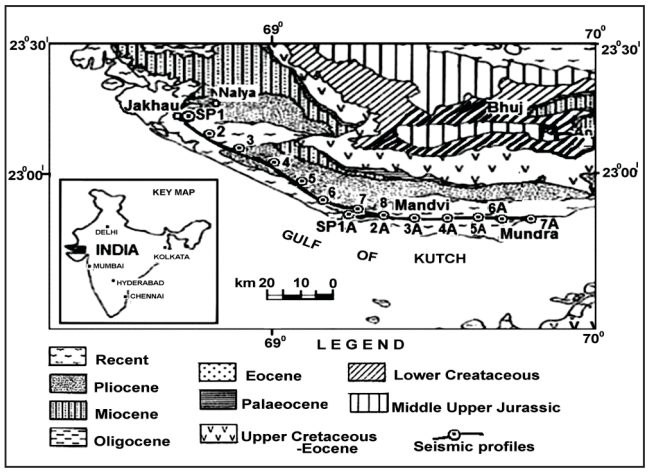

Fig. 1: Location of seismic profiles on geology map of Kutch basin (Courtesy, NGRI Technical Report No.NGRI-2000-EXP-296).

three important Precambrian tectonic trends of Delhi, Aravalli and Satpura. According to Biswas (1987), these rifting events are synchronous with the major events in India's drift history.

Modeling of seismic data

To gain advantage of inversion, 2-D travel time inversion of Zelt and Smith (1992) was applied to the first arrivals and identifiable reflected phases from all shots along 72 km long Jakhau-Mandvi (NW-SE) profile, and 57 km long Mandvi-Mundra (W-E) profile with a view to build basement configuration and delineate overlying sedimentary formations along the two profiles. The forward computation to the ray based inversion is based on efficient ray tracing equations (Zelt and Ellis, 1988). The data are assigned with uncertainties of 50 ms. The assignment of uncertainties is subjective and is based on one period of dominant frequency (20 Hz) of the data. The model is parameterized by linear interpolation between an irregular grid of boundary nodes and upper and lower layer velocity nodes. A smooth layer boundary simulation is used to avoid scattering and focusing of ray paths and to stabilize inversion. The travel times and their partial derivatives with respect to velocity and boundary nodes are calculated during the ray tracing. The calculated response of the model is compared with the observed data, and the model parameters are updated using the correction vector obtained from the damped least-squares inversion (Zelt and Smith, 1992; Zelt, 1999). The process is repeated until, achieved a satisfactory fit corresponding to a normalized χ^2 value of nearly 1. However, it is not always possible to obtain χ^2 =1 while maintaining acceptable resolution of model parameters because of data sampling at small-scale heterogeneities that cannot be resolved by modeling (Zelt, 1999). Adding more nodes will typically reduce the travel time residual, but decrease the parameter resolution. Therefore, we build a minimum structure velocity model defined by few parameters. This represents the true structure (O, Leary et al. 1995) and results are free from modeling artifacts. It is to be stated that the final velocity model was derived based on the ability to trace rays through the final model to almost all observations and a trade-off between achieving a sufficiently small travel time residual of the order of data uncertainties and an adequately high parameter resolution. The ray diagram and final velocity models showing the low-velocity Mesozoics below the basalt cover are shown in Figs 2 and 3. The data were fitted with rms travel time residuals of 57 ms and 58 ms corresponding to normalized χ^2 values of 1.29 and 1.34 for the Jakhau-Mandvi and Mandvi-Mundra profiles, respectively. The modeling is done in a layer-by-layer fashion.

Merely fitting the observed data is not adequate for modeling. An important aspect is to provide a measure of resolution and uncertainties of estimated model parameters from the diagonal elements of the resolution and covariance matrices respectively. The inversion parameters are 1.0 for the overall damping factor, 0.10 km/s for a priori uncertainty in velocity parameter and 0.15 km for a priori uncertainty in depth parameter. The resolution values range from 0 to 1 and the parameters associated with values more than 0.5 are considered reasonably resolved. The resolution of most of the velocity and depth nodes along the two profiles are more than 0.6 but less than 0.85, indicating that the model has been well resolved. Since we have good ray coverage (Figs 2b and 3b) in large part of the model, the resolution is good for all nodes except to those near the end of the profiles. The standard deviations, calculated from covariance matrices, represent the statistical errors associated with various model parameters. To account for the non-linearity of the travel time inversion and to provide absolute uncertainty, we have performed the uni-parameter uncertainty test (Zelt and Smith, 1992; Zelt, 1999). To save the modeling time we have estimated the absolute uncertainties at selected velocity (solid circles) and boundary (squares) nodes (shown in Figs 2c and 3c) along the profiles. The uncertainty of the basalt velocity is estimated as 5.3± 0.09 km/s (bounding between 5.22 km/s to 5.39 km/s) and that of the basement depth is

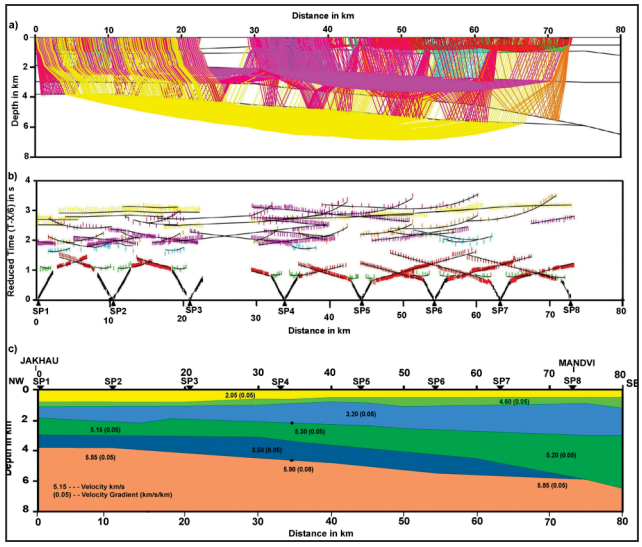

Fig. 2: a) Ray diagram and b) observed (vertical bars) and calculated (lines) travel times through derived velocity model from eight shots used in the inversion. Colors represent various phases of refractions and reflections, and corresponding rays. c) 2-D velocity structure along Jakhau-Mandvi profile exhibiting Mesozoic sediment (3.20 km/s) below the Deccan basalt (4.50-4.80 km/s).

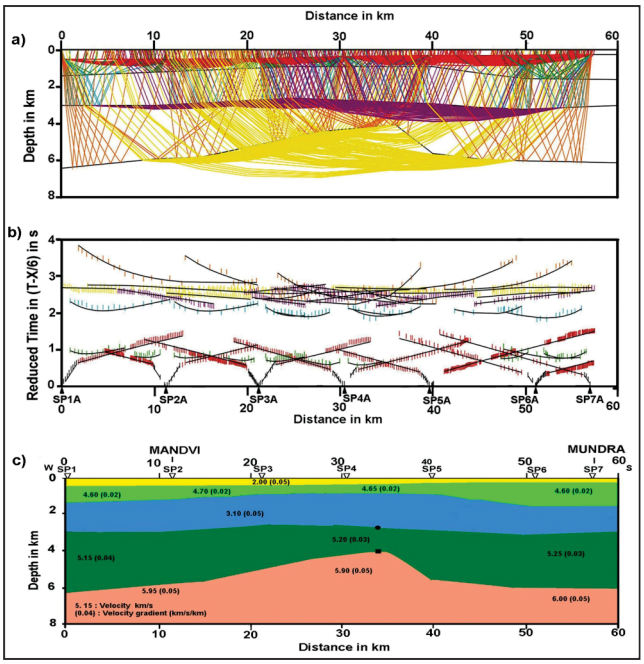

Fig. 3: (a) Ray diagram and b) observed (vertical bars) and calculated (line) travel times through derived velocity model from seven shots used in the inversion. Colors represent various phases of refractions and reflections, and corresponding rays. c) 2-D velocity structure along Mandvi-Mundra profile exhibiting Mesozoic sediment (3.20 km/s) below the Deccan basalt (4.60-4.80 km/s).

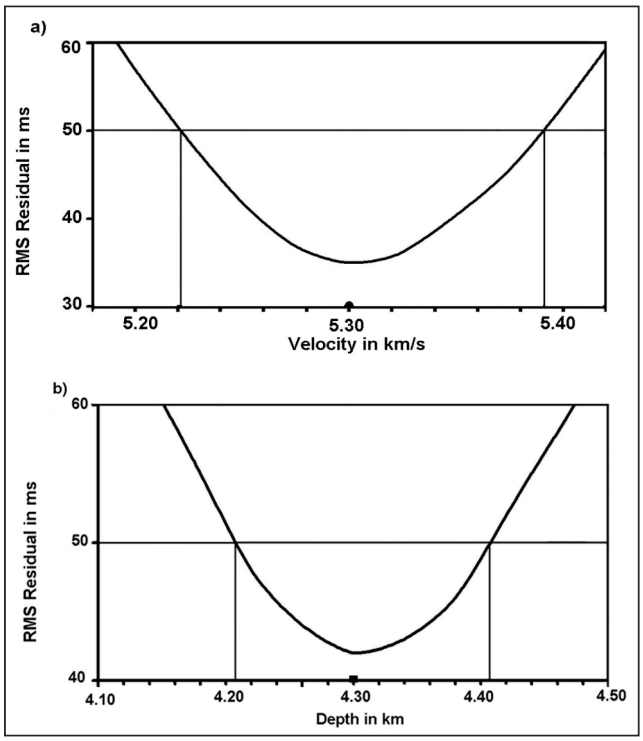

Fig. 4: a) Root Mean Square (RMS) travel time residual as a function of velocity perturbation for the velocity node (circle) of basalt layer; b) Root Mean Square (RMS) travel time residual as a function of depth perturbation for the boundary node (square) along the Jakhau-Mandvi profile. The velocity and depth corresponding to 50 ms travel time residuals represent the lower and upper bounds of the velocity and depth nodes, respectively.

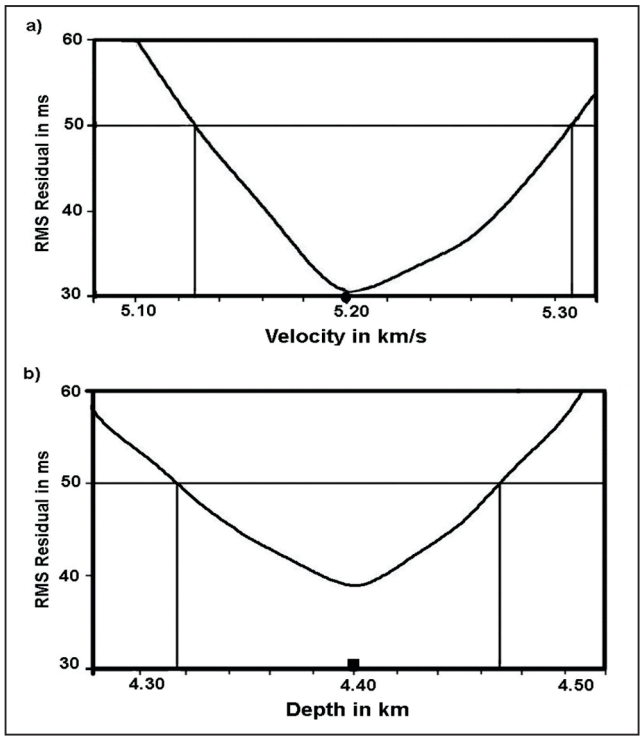

Fig. 5: a) Root Mean Square (RMS) travel time residual as a function of velocity perturbation for the velocity node (circle) of basalt layer; b) Root Mean Square (RMS) travel time residual as a function of depth perturbation for the boundary node (square) along the Mandvi-Mundra profile. The velocity and depth corresponding to 50 ms travel time residual represent the lower and upper bounds of the velocity and depth nodes, respectively.

estimated as 4.3±0.10 km (lying between 4.21 km to 4.41 km), each corresponding to 50 ms travel time residual along the Jakhau-Mandvi profile (Fig.4). Whereas, the uncertainty of the basalt velocity is estimated as 5.2±0.09 km/s (bounding between 5.13 km/s to 5.31 km/s), and that of the basement depth is estimated as 4.4±0.08 km (lying between 4.32 km to 4.47 km), each corresponding to 50 ms travel time residual along the Mandvi-Mundra profile (Fig.5).

Gravity modeling

To assess whether the seismically derived velocity structure can explain other geophysical data, performed gravity modeling along the two lines. For gravity modeling, converted the derived seismic velocity models into initial density models using the velocity-density relationship of Nafe and Drake (1957) and Ludwig et al. (1970). The layers of the P-wave velocity model define respective layers of the gravity model. The densities are then marginally adjusted to match the observed gravity data as closely as possible using the forward modeling approach of Zelt (1989) based on gravity algorithm of Talwani et al. (1959).

The gravity data along the Jakhau-Mandvi and Mandvi-Mundra profiles have been taken from the Bouguer gravity anomaly map (NGRI Technical Report no.NGRI-2000-EXP-296) of the southern part of the Kutch Basin. The residual Bouguer anomaly (Fig.6a) along the Jakhau-Mandvi profile

shows a large wave length gradient decreasing from NW to SE and it is superimposed by several small wavelength lows and highs, which represent local/shallower features. The large wavelength residual Bouguer anomaly decreases towards SE (Mandvi) with two gravity lows (L1 and L2) at 47 and 74 km profile distance. The final gravity model (Fig.6b) presents a five-layer model with densities of 2.07, 2.74, 2.36, 2.55, 2.40 g/cc overlying the basement with density of 2.70 g/cc. The subsurface density model with thickening of sedimentary column towards SE of the profile, corroborates further the work of Chandrasekhar and Mishra (2002).

The residual Bouguer anomaly (Fig.7a) along the Mandvi-Mundra profile shows two gravity lows (L2, L3) on either side with high anomaly in the center. The subsurface density model (7b) consists of four layers with densities 2.05, 2.71, 2.32 and 2.56 g/ccunderlain by a basement with density of 2.69 g/cc. The basement and the overlying sediments are uplifted in the center suggesting an anticlinal structure, and faulted basement at ~35 km along the profile. The gravity lows (L2, L3) representing the depressions on either side of the uplift are primarily caused due to sediments. The uplift coincides with the N-S extending Median High reported in this region from the geological studies (Biswas, 1987).

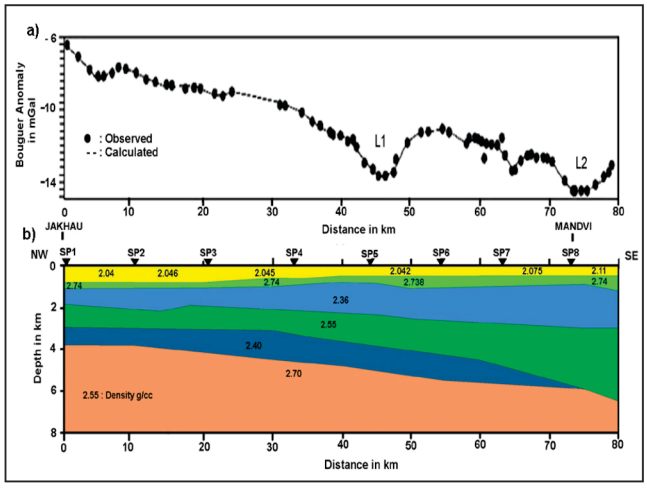

Fig. 6: Density model along the Jakhau-Mandvi profile.

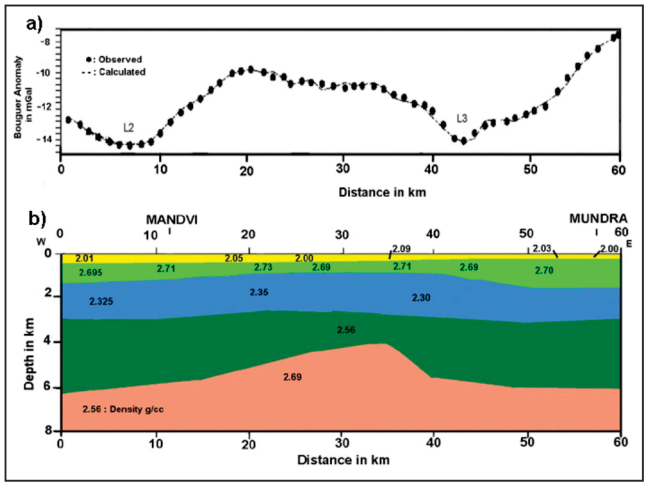

Fig. 7: Density model along Mandvi-Mundra profile.

Results and Discussions

The estimated velocity structure is an improved version compared to earlier models (NGRI Technical Report no. NGRI-2000-EXP-296 and Prasad et al., 2010), as the present model has taken into consideration both the first arrival refraction and later arrival wide angle reflection data. Besides, the present study has provided a measure of resolution and uncertainty of the estimated model parameters without which the modeling is not complete. Again, the seismically derived structures have been assessed by gravity modeling that has yielded a better configuration by filling the gaps in seismic data.

By comparing the velocity structure with the litholog available from Suthri well (Fig.8), it is suggested that the velocity layers from surface downward correspond to the Tertiary sediments, Late Cretaceous Deccan basalt, Early Cretaceous sediments, Late Jurassic Limestone and Early Jurassic sediments, in succession above the Archean basement.

The thickness of the Tertiary sediments with velocity of 2.0 km/s and average density of 2.05 g/cc varies between 850 m in the NW part of the profile to 500 m in the SE part along the Jakhau-Mandvi profile. The second layer with velocity of 4.6 km/s and density of 2.73 g/cc is associated with the Deccan basalt, the thickness of which varies between 250 m to 600 m from NW to SE direction. Underlying this layer lies the low velocity (3.2 km/s) and low density (2.23g/cc) Early Cretaceous sediments. The thickness of this layer increases SE direction, reaching the maximum value of ~2000 m at the

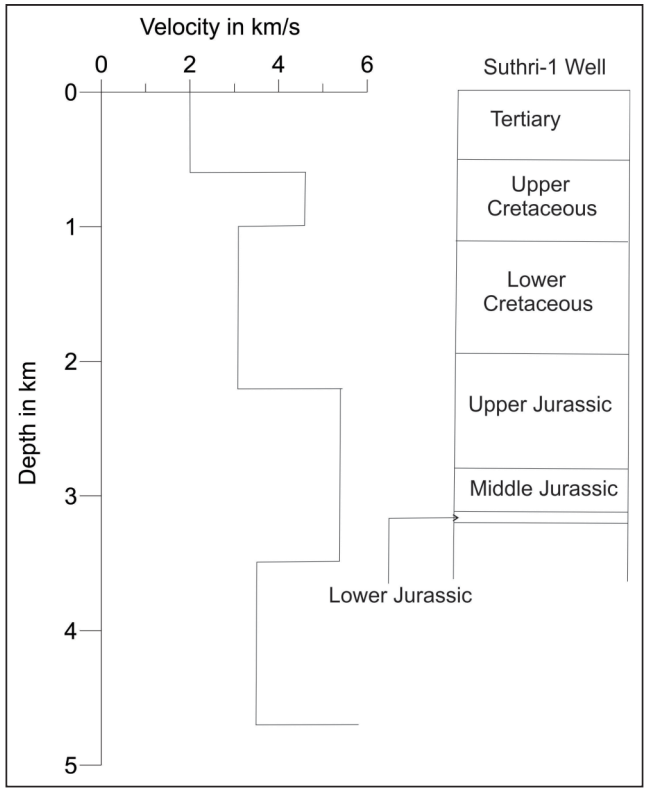

Fig. 8: Suthri well: Interval velocity with lithological information (After, ONGC).

end of the profile. The low velocity/density sedimentary layer is underlain by a high velocity (5.2 km/s) and high density (2.55 g/cc) layer, representing the Late Jurassic Limestone. The thickness of the Limestone is found to increase from 1000 m in the NW segment to 2800 m in the SE segment of the profile. This layer is underlain by another low-velocity (3.5 km/s) and low density (2.40g/cc) layer corresponding to the Early Jurassic sediments. It exhibits a truncated structure in the SE segment of the profile near Mandvi. It is to be stated that we cannot categorically delineate the truncation point from the wide-angle seismic data. The last layer is the Archean basement with velocity of 5.9 km/s and density of 2.70 g/cc, and deepens from 3800 m in NW to 5750 m in SE.

The Early Jurassic sediments, delineated along the Jakhau-Mandvi profile, are not observed along the Mandvi-Mundra profile. The thickness of the top Tertiary sediments with velocity of 2.0 km/s and density of 2.05 g/cc varies between 200 m in the east to 500 m in the west. The second layer (Deccan basalt) with velocity of 4.65 km/s and average density of 2.71 g/cc is thicker along this profile than that along the Jakhau-Mandvi profile. This layer thickens on either side of the profile, reaching to the maximum value of 1.5 km near Mundra. The third layer with velocity of 3.1 km/s and average density of 2.325 g/cc, representing the low velocity Early Cretaceous sediments, is quite thick (more than 1.6 km) throughout the profile compared to that in the Jakhau-Mandvi profile with little broader (~ 2.0 km) in the middle. The next layer with velocity of 5.2 km/s and density of 2.56 g/cc is also thicker than that in the Jakhau-Mandvi profile. However, it thickens to 3.2 km on either side from the middle (1.5 km) of the profile. This is underlain by the Archean basement (5.95 km/s velocity and 2.69 g/cc density), which shows an uplift near 35 km profile distance with its impact on the overlying sedimentary formations. This coincides with the N-S extending Median High reported by Biswas (1987) from the geological studies in the Kutch basin.

Conclusions

Inversion of first arrival refraction and wide angle reflection travel time data has yielded a complex large-wavelength velocity model. The five layers along the Jakhau-Mandvi profile may represent the Tertiary, Late Cretaceous Deccan basalt, Early Cretaceous sediments, Late Jurassic Limestone and Early Jurassic sediments below the Archean basement, which is about 3.7 km deep below Jakhau and deepens further to a depth of 6.4 km near Mandvi. The early Jurassic sediments along the Jakhau-Mandvi profile pinches out near Mandvi, and is not observed along the Mandvi-Mundra profile. The large thickness of Mesozoic sediments is a manifestation of extensional regime prevailing during the Mesozoic rifting. The gravity model also suggests the presence of large thickness of sediments in the Kutch Basin. An uplift in the basement and overlying sedimentary formations indicates an anticline structure in the middle of the Mandvi-Mundra profile. This coincides with the N-S extending Median High that has been reported in the Kutch region from geological studies.

Acknowledgements

The authors thank the Director, NGRI for permission to publish this paper. Thanks are also due to Dr. P. R. Reddy for his valuable suggestions to improve the quality of the manuscript. This is a contribution to SHORE Project of NGRI under the 12th Five Year Plan of CSIR.

References

Besse, J. and Courtillot, V., 1988. Paleogeographic maps of the Indian Ocean bordering continents since the early Jurassic, J. Geophys. Res., 93, 11791-11808.

Biswas. S.K., 1982. Rift basins in western margin of India and their hydrocarbon prospects with special reference to Kutch basin, The American Association of Petroleum Geologists, 66 (10), 1497-1513.

Biswas, S.K., 1987. Regional tectonic framework, structure and evolution of the western marginal basins of India, Tectonophysics, 135, 305-327.

Chandarsekhar. D.V. and Mishar.D.C., 2002. Some geodynamic aspects of Kutch basin and seismicity: an insight from gravity studies. Current Science, 83(4), 492-498.

Ludwig, W. J., Nafe, J. E., and Drake, C. L., 1970. Seismic refraction, in The Sea, vol. 4, part 1, New Concepts of Sea Floor Evolution, edited by A. E. Maxwell, pp. 5384, Wiley-Interscience, Hoboken, N. J.

Malik, J.N, Sohoni, P.S., Merh, S.S., Karanth, R.V., 2000. Palaeoseismology and neotectonism of Kachchh, western India. In: Okumura, K., Goto, H., Takada, K (Eds.), Active Fault Research for the New Millennium, Proceedings of the Hokudan International Symposium and School on Active Faulting. pp. 251-259.

Nafe, J. E., and Drake, C. L., 1957. Variation with depth in shallow and deep water marine sediments of porosity, density and the velocities of compressional and shear waves, Geophysics, 22, 523-552.

National Geophysical Research Institute (NGRI), 2000, Integrated geophysical studies for hydrocarbon exploration, Kutch, India: Hyderabad, India, Technical Report NGRI-2000-EXP-296, 195 p.

O'Leary, D.M., Ellis, R.M., Stephenson, R.A., Lane, L.S. & Zelt, C.A., 1995. Crustal structure of the northern Yukon and Mackenzie Delta, north-western Canada, J. Geophys., Res., 100(B7), 9905-9920.

Prasad, B.R., Venkateswarlu, N., Prasad, A.S.S.S.R.S., Murthy, A.S.N. and Sateesh, T., 2010. Basement configuration of on-land Kutch basin from seismic refraction studies and modeling of first arrival travel time skips, Jour. Asian Earth Sciences, 39, 460-469.

Rayamp-PC, 1987. 2D Ray Tracing/Synthetic Seismogram, Version 2.1, Geophysics Laboratory, Mc-Gill University.

Sain, K. and Reddy, P.R., 1995. Direct calculation of thicknesses of high velocity and underlying low velocity layers using post-critical reflection times in seismic refraction experiments, Jour. of App. Geophys., 134, 125-136.

Sain, K. and Kaila, K.L., 1996. Ambiguity in the solution of the velocity inversion problem and a solution by joint inversion of seismic refraction and wide-angle reflection times, Geophys. Jour. Int., 124, 215-227.

Sain, K., Zelt, C.A. and Reddy, P.R., 2002a. Imaging subvolcanic Mesozoics using travel time inversion of wide-angle seismic data in the Saurashtra peninsula of India, Geophys. Jour. Int., 150, 820-826.

Sain, K., Reddy, P.R. and Behera, L., 2002b. Imaging of low-velocity Gondwana sediments in the Mahanadi delta of India using travel time inversion of first arrival seismic data, Jour. of App. Geophys., 49, 163-171.

Sridhar, A.R., Prasad, ASSRS, Satyavani, N. and Sain, K., 2009. Sub-Trappean Mesozoic sediments in the Narmada basin based on traveltime and amplitude modeling - a revisit to old seismic data, Current Sciences, 97, 1462-1466.

Srinivas, Khar, 1995. Exploration of Frontier basins and hydrocarbon prospects. Petrotech-95 1, 319.

Talwani, M., Worzel, J. L., and Landisman, M. G., 1959. Rapid gravity computations for two-dimensional bodies with application to the Mendocino submarine fracture zone, J. Geophys. Res., 64, 49-59.

Zelt, C. A., and Ellis, R. M., 1988. Practical and efficient ray tracing in 2-D media for rapid travel time and amplitude forward modeling, Can. J. Explor. Geophys., 24, 16-31.

Zelt, C.A. and Smith, R.B., 1992. Seismic travel time inversion for 2-D crustal velocity structure, Geophysical Journal International, 108, 16-34.

Zelt, C.A., 1989. Seismic structure of the crust and upper mantle in the Peace River Arch region, Ph.D. thesis, University of British Columbia, Vancouver.

Zelt, C.A., 1999. Modeling strategies and model assessment for wide-angle seismic traveltime data, Geophys. J. Int. 135, 1101-1112.